Applied Surface Science 420 (2017) 586–593

Contents lists available at ScienceDirect

Applied Surface Science

journal homepage: www.elsevier.com/locate/apsusc

Full length article

Hydrogenated amorphous carbon films on steel balls and Si substrates: Nanostructural evolutions and their trigging tribological behaviors

Yongfu Wang[a,1], Yan Wang[b,1], Xingkai Zhang[a], Jing Shi[a], Kaixiong Gao[a], Bin Zhang[a,*], Junyan Zhang[a,*]

[a] State Key Laboratory of Solid Lubrication, Lanzhou Institute of Chemical Physics, Chinese Academy of Sciences, Lanzhou 730000,& China and University of Chinese Academy of Sciences, Beijing 100049, China
[b] School of Petrochemical Technology, Lanzhou University of Technology, Lanzhou,730050, China

ARTICLE INFO

Article history:
Received 21 March 2017
Received in revised form 10 May 2017
Accepted 20 May 2017
Available online 22 May 2017

Keywords:
Hydrogenated amorphous carbon film
Graphite-like
Fullerene-like
Super-low friction
Wear

ABSTRACT

In this study, we prepared hydrogenated amorphous carbon films on steel balls and Si substrates (steel ball- and Si substrate-films) with different deposition time, and discussed their carbon nanostructural evolutions and tribological behaviors. The steel ball-film structure started to be graphite-like structure and then gradually transformed into fullerene-like (FL) structure. The Si substrate-film structure began in FL structure and kept it through the thickness. The difference may be result from the competition between high starting substrate temperature after additional nitriding applied on the steel balls (its supply power is higher than that in the film deposition), and relaxation of compressive stress from energized ion bombardment in film deposition process. The FL structural film friction couples could achieve ultra-low friction in open air. In particular, the Si substrate-film with 3 h, against the steel ball-film with 2 h and 3 h, exhibited super-low friction (~0.009) and superlong wear life (~5.5×10^5 cycles). Our result could widen the superlubricity scope from previously high load and velocity, to middle load and velocity.

1. Introduction

Amorphous hydrogenated carbon (a-C:H) films have been emerged and well developed, due to their extraordinary properties of high mechanical hardness and low friction coefficient [1,2]. The atomic-bond structure of such films can be deduced from their Raman spectra, which are dominated by two vibrational modes at 1360 (*D*-mode) and 1560 cm^{-1} (*G*-mode) [3]. The D and G bands must usually be assigned a frequency of vibration to achieve a good Raman fit quality. However, the fitting discrepancy has been reported [4–6]. It most likely originates from the structure inhomogeneity due to the presence of some topological defects such as pentatomic and heptatomic rings [4,6]. Recently, the a-C:H films with a fullerene-like (FL) structure containing high volume of odd rings have been already synthesized [7,8]. Such films' preparation methods, additional element or carbon nanostructure incorporations, and mechanical properties as well as frictional behaviors have been investigated [7–16]. Nevertheless, the structure inhomogeneity or evolution throughout the thickness of the FL structural film is scarcely reported, and its trigging friction benefit is not known. In addition, the nature of underlying substrate material causes the film structure even more complex at a starting deposition. Thus, it is very necessary to study the structural change throughout the thickness and detect its triggering tribological behavior.

In this study, we have prepared two groups of a-C:H films on steel balls and Si substrates (steel ball- and Si substrate-films) with different deposition time. Due to the weak adhesion of steel to carbon, we employ additional plasma nitriding pre-process by in-situ depositing a FeN intermediate layer. At the starting film deposition (0.5 h), graphite-like (GL) structure is formed on steel ball surface whereas FL structure appears in the Si substrate-film. The difference may be due to higher steel ball temperature from additional plasma nitriding (because the supply power of the film deposition deceases after the nitriding). With the increasing time, the steel ball-film structure gradually transforms from GL structure to FL structure. The transformation may be result from higher steel ball temperature and relaxation of high compressive stress from energized ion bombardment in the film deposition (because

* Corresponding authors.
E-mail addresses: bzhang@licp.cas.cn (B. Zhang), zhangjunyan@licp.cas.cn (J. Zhang).
[1] The two authors contributed equally to this paper.

http://dx.doi.org/10.1016/j.apsusc.2017.05.169
0169-4332/

the stress relaxation can arise from the formation of pentatomic and heptatomic rings). We also investigate their frictional behaviors between the steel ball-films and Si substrate-ones. The FL structural film friction couples can achieve ultra-low or super-low friction in open air. In particular, the Si substrate-film with 3 h, against the steel ball-film with 2 h and 3 h, exhibit super-low friction (~0.009) and superlong wear life (~5.5×10^5 cycles). Zhang et al. [9,13] have reported that FL hydrogenated carbon film synthesized by plasma-enhanced chemical-vapor deposition technique, exhibit ultra-low or super-low friction under high load and velocity (15–20 N and ≥0.12 m/s) in ambient conditions with 20% relative humidity. Fullerene-like MoS_2 nanoparticle film has shown to attain superlubricity in nitrogen and 45% humidity (10 N, 0.5 m/s and a hertzian pressure of 1.1 GPa) [17]. Our result can widen the scope of attaining super-low friction in open air, for the FL film couples have moderate test condition such as middle load and velocity (5 N, and 0.05 m/s).

2. Experimental

The surfaces for steel balls (⌀5) and Si substrates were etched by Ar^+ (negative voltage of 1000 V, pulsed frequency: 80 kHz and duty cycle of 0.8). The a-C:H films were prepared by a DC-pulsed plasma chemical-vapor deposition (PECVD) system with supply power (negative voltage of 1000 V, pulsed frequency: 75 kHz and duty cycle of 0.5), mixed gas of methane and hydrogen with a partial pressure ratio of 2:1, and different deposition time (0.5 h, 1 h, 1.5 h, 2 h, 2.5 h and 3 h). The films on steel balls were named as 0.5 h/Fe ball, 1 h/Fe ball, 1.5 h/Fe ball, 2 h/Fe ball, 2.5 h/Fe ball and 3 h/Fe ball samples. The films on Si substrates were referred as 0.5 h/Si, 1 h/Si, 1.5 h/Si, 2 h/Si, 2.5 h/Si and 3 h/Si samples. The additional plasma nitriding pre-process was used on steel balls after Ar^+ etching and before the film deposition. It had the deposition conditions: (1) negative voltage: 1200 V; (2) pulsed frequency: 80 kHz; (3) duty cycle: 0.8; (4) gas flow rate: N_2 = 90 SCCM; (5) depositing time: 2 h. Transmission Electron Microscopy (TEM, FEI Tecnai F30, FEI, Eindhoven, The Netherlands), X-ray photoelectron spectroscopy (XPS, operating with Al-Ka radiation and detecting chamber pressure of below 10^{-6} Pa) (Physical Electronics Inc., USA), micro-Raman analyses (Jobin-Yvon HR-800, Horiba/Jobin Yvon, Longjumeau, France) and Reflection fourier-transform infrared (FTIR) measurement (Nexus 870) were employed to reveal the films' microstructures. The TEM samples about 20 nm thickness were grown on freshly cleaved NaCl wafers (single crystals) under the film deposition condition, and then dissolved with distilled water and placed on Cu grids. Prior the XPS detection, the Au thin films about 0.2 nm thickness were deposited on the film surfaces, which minimizes the charging effect, and helps to detect the changes of C ls peaks. The frictional behaviors of the couples, namely, the Si substrate-films against the steel ball-films, were assessed on a reciprocating ball-on-disc tribotester with a relative humidity (RH) of about 25%. All tests were performed under a load of 5 N, an amplitude of 5 mm, and a frequency of 5 Hz. A comparative a-C:H film on a Si substrate was produced using the same deposition method (bias voltage 500 V, CH_4 30 SCCM, and working gas pressure 27 Pa).

3. Results and discussion

3.1. Overview of basic properties of the samples

In this study, we focus on the structure inhomogeneity or evolution throughout the thickness of the fullerene-like (FL) structural a-C:H film. Thus, the 3 h/Si sample is chosen as a representative to study the structure properties of these films. The curved graphite layers observed in the sample are a typical FL feature (Fig. 1(a)) [9,18]. The observed curvature is due to the production of both pentagons and heptagons distributed randomly throughout a hexagonal network as C_{60}. The layers aren't present in the comparative a-C:H film (Fig. 1(b)). Besides, the additional Raman peaks at ~710, 860 and 1200 cm^{-1} compared with the comparative a-C:H film can be assigned to the curvature in graphitic planes and carbon nano-onions, as has been confirmed in other reports [7,13] (Fig. 1(c)). The sample has rich sp^2-bonded carbon mixture, confirmed via FTIR, due to the presence of a strong absorption peak centered at ~1600 cm^{-1} in the range of 1520–1700 cm^{-1} (Fig. 1(d)). The peak at 1580 cm^{-1} due to the G band in graphite, and the 1640 cm^{-1} peak attributed to sp^2-bonded carbon in olefinic chain, are in the range [2,19]. The presence of sp^2 carbon mixtures is supported by the XPS results that the sample's C 1*s* core position is close to that of graphite (284.3 eV) compared to the comparative a-C:H film(Fig. 1(e)). Based on the detected results, the 3 h/Si sample has a typical FL character.

3.2. Characteristics of the samples on steel balls with depositing time

Raman spectroscopy is a surface detection system, which is considered to distinguish different microstructures in carbon based films [3]. In the early Raman fit model, G (graphitic) and D (disorder induced) bands are used to fit a-C spectra based on the active vibrational modes of disordered nanocrystalline graphite, or glassy carbon [3]. The I_G/I_D is used to estimate the ratio of sp^3 and sp^2 bondings. Nevertheless, the model fails to distinguish topological defects or nanoclusters. Recently, the four peaks' fit method is suggested to recognize carbon ring clusters [4,6,7,14], which involves A_{1g} at 1360 cm^{-1} and E_{2g} at 1569 cm^{-1} for six C-atom rings, A_{1g} at 1470 cm^{-1} for pentagons, and A_{1g} at 1200 cm^{-1} for heptagons. The origin and variation of the fit method have been discussed in a manner described elsewhere [4,6,7,14]. For pure carbon structures, curvature of graphite basal planes is induced by the incorporation of pentagons and heptagons in a hexagonal network. Therefore, the fraction of pentagons and heptagons is an indicative for FL content change to a certain extent.

Fig. 2 shows the four peaks' fit results of the samples on steel balls with different deposition time. At 0.5 h, the sample exhibits a Raman character different from the comparative a-C:H film (green line in Fig. 2(a)) which has a one bulging peak at ~1510 cm^{-1}. It is noted that the D peak (at ~1380 cm^{-1}) can be distinguished as broad shoulders or as local maximums in the sample's spectrum, and the G peak position is ~1555 cm^{-1}. Thus, the 0.5 h/Fe ball spectrum looks like that of graphite (blue line in Fig. 2(a)) which has two isolated D peak (at ~1350 cm^{-1}) and G peak (at ~1560 cm^{-1}). Moreover, compared with the other steel ball-samples (Fig. 2(b)-(f)), the 0.5 h/Fe ball spectrum shows a different profile. Its G peak obviously shifts towards higher wave numbers, for example, than 1527 cm^{-1} of the 3 h/Fe ball sample. Therefore, the 0.5 h/Fe ball sample has a graphite-like (GL) character. When the deposited time increases from 0.5 h to 1.5 h, the weak D shoulder peak (at ~1380 cm^{-1}) observed at 0.5 h/Fe ball sample gradually disappears, and the G peak position decreases from ~1555 cm^{-1} to ~1541 cm^{-1}(Fig. 3). The 1 h/Fe ball and 1.5 h/Fe ball spectra are fitted into four peaks with Gaussian line shapes. The peaks from pentagons (at ~1470 cm^{-1}) and heptagons (at ~1200 cm^{-1}) can be more obviously observed. The changes mean topological defects such as odd ring clusters are progressively formed in the GL layer, bond angle distortion and other disorders cause a softening of the vibration frequencies, and the GL clusters become smaller and their layers develop curvature. Namely, at this stage, the 1 h/Fe ball and 1.5 h/Fe ball films gradually own curved graphite layer features, i.e. FL elements.

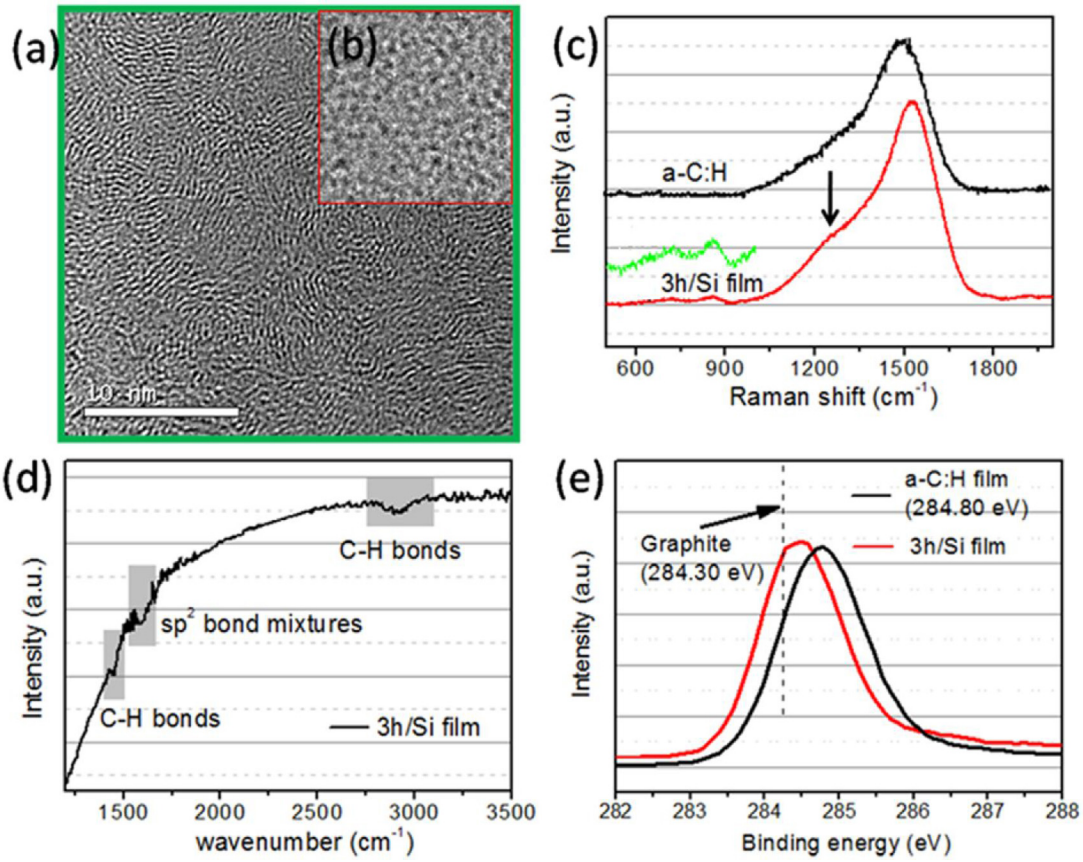

Fig. 1. TEM (a), FTIR (c), Raman (d) and XPS (e) results of the 3 h/Si sample. The set (b) shows TEM image of a comparative a-C:H film.

When the deposited time increases to 2 h, a weak and isolated peak at ~1200 cm^{-1} can be observed. The peak can be assigned to the curvature in graphitic planes and carbon nano-onions as has been confirmed in other reports [7,13]. Thus, FL structure is further growth which is supported by the highest fraction of pentagons and heptagons at 2 h (Fig. 3). As increase to 3 h, FL content slightly decreases. Overall, the steel ball-films' structure gradually transforms from GL structure to FL structure, and FL content increases more quickly at the early deposition and then keeps relative stable.

Raman spectrum reflects film surface nature and it is difficult to recognize film bulk nature, because Raman spectroscopy has a limit of probing depth of 50–100 nm for visible excitation. In order to get the information of the samples' bulk nature, reflection FTIR spectra are invoked to further confirm the structural changes above. The samples have two weak peaks of C-H absorption at ~1450 and ~2950 cm^{-1}, and a strong absorption peak at 1600 cm^{-1} from sp^2 carbon mixtures (Fig. 4). For 0.5 h/Fe ball sample, its three peaks look weaker than that of the other samples. This is associated with the thinnest thickness of the 0.5 h/Fe ball sample. Thus, the spectrum at 0.5 h thereby fails to reflect the transformation from GL structure to FL structure. At 1 h and 1.5 h, the 1600 cm^{-1} peak can be more clearly recognized. This probably results from the increasing of their thickness. As the depositing time increases from 2 h to 3 h, the 1600 cm^{-1} peak become weaker, coincide with the gradual disappearance of GL structure throughout the thickness. The GL disappearance throughout the thickness accompanies with the G peak towards lower wave numbers, which means that the fraction of sp^2 bonded carbon deceases. This is supported by the strengthening of C-H peaks at over 2 h. The higher hydrogen surrounding can be partly attributed to the structural changes, because hydrogen atoms during the depositing process can preferentially etch the sp^2 phase and destroy GL structures to some extent [2].

3.3. Characteristics of the samples on Si substrates with deposition time

Fig. 5 shows Raman spectra and corresponding fit results of the Si substrate-samples. We note that these spectra are different from that of the steel ball-films. Firstly, the 0.5 h/Si spectrum is inconsistent with the 0.5 h/Fe (blue line in Fig. 5) and 1 h/Fe ball (Fig. 2) ones, and similar to the spectra on Fe balls over 1.5 h. Its odd ring fraction (~25%) is higher than those of the 0.5 h/Fe (few content due to the presence of GL structure) and 1 h/Fe ball ones (~21.4%) (Fig. 6). This indicates that the 0.5 h/Si sample crosses the stage of forming GL clusters, and goes directly to a stage of forming FL structure. This is supported by the FL nucleation on Si substrates for FL based carbon films [20,21]. FL-CNx film has two possibilities: nucleation directly on a Si substrate surface, or nucleation at distance of about 2 nm from the substrate [20]. For FL-C:H film, FL clusters nucleates about ~10–30 nm from a Si substrate surface [21]. Moreover, our 0.5 h/Si sample's thickness is ~160 nm (Fig. 7), which is more than the probing depth limit (50–100 nm) and nucleation distance from Si substrate surface. Secondly, all the Si samples exhibit a typical FL character and remain relatively higher FL fraction (Fig. 6). This shall be due to the FL formation directly at the starting deposition. Finally, a maximum FL content is achieved at the 1.5 h/Si sample (Fig. 6), whereas the steel ball-sample reaches a maximum value at 2 h (Fig. 3). Overall, the Si substrate-films' structure directly evolves towards FL formation, unlike the steel ball-films in which odd ring clusters are progressively formed in the GL layers, and their layers develop curvature to form FL clusters.

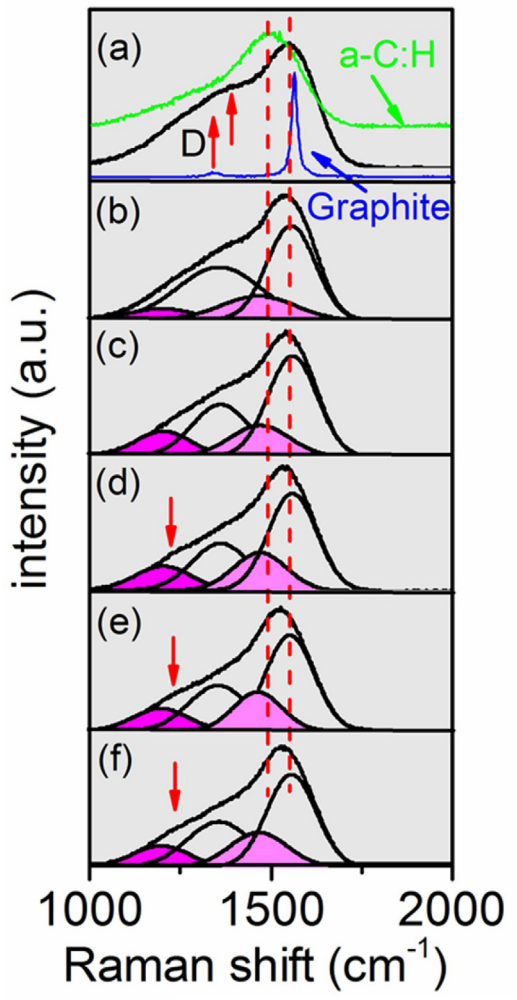

Fig. 2. Raman spectra and their fit results of the samples on steel balls with different deposition time, 0.5 h/Fe ball (a), 1 h/Fe ball (b), 1.5 h/Fe ball (c), 2 h/Fe ball (d), 2.5 h/Fe ball (e) and 3 h/Fe ball (f).

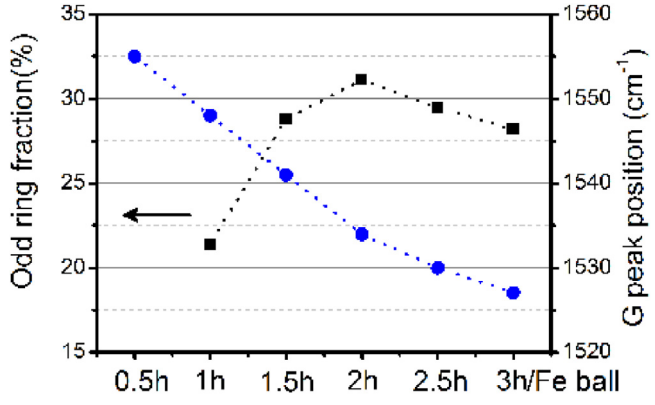

Fig. 3. odd ring fraction and G peak position of the samples on steel balls with depositing time.

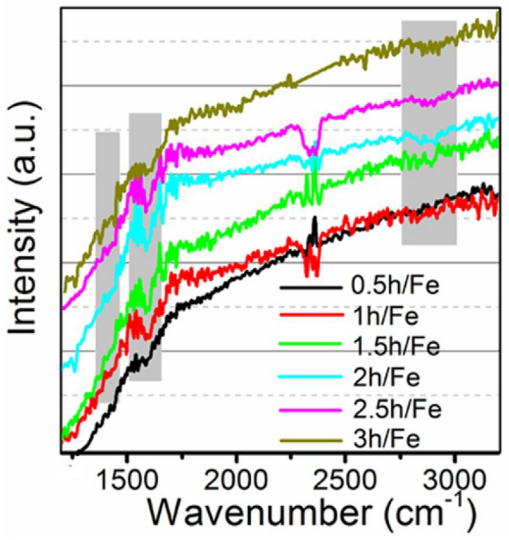

Fig. 4. FTIR results of the samples on steel balls with different deposition time.

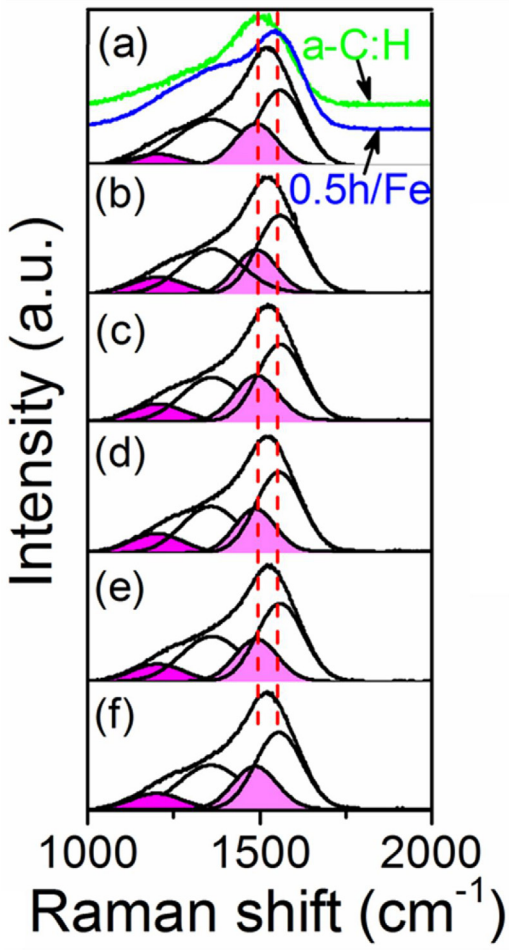

Fig. 5. Raman results of the samples on Si substrates with different deposition time, 0.5 h/Si (a), 1 h/Si (b), 1.5 h/Si (c), 2 h/Si (d), 2.5 h/Si (e) and 3 h/Si (f).

According to the 3.2 section, reflection FTIR spectrum fails to reveal the structural change when the detected sample is too thin. Because the steel ball-films' thickness is difficult to be measured, the thickness of the Si substrate-samples as a function of deposition time are shown in Fig. 7. The thickness looks like to increase more quickly at the early deposition than at the late stage. Fig. 8 shows FTIR results of the samples. The two C-H peaks at 1450 and 2950 cm^{-1} and the peak at 1600 cm^{-1} from sp^2 bond mixtures are difficult to be recognized at 0.5 h/Si and 1 h/Si sample. These peaks can be observed until the 1.5 h/Si sample has a thickness of ~560 nm. The FTIR difference between the steel ball-films and Si substrate-ones may be due to their substrate materials and their

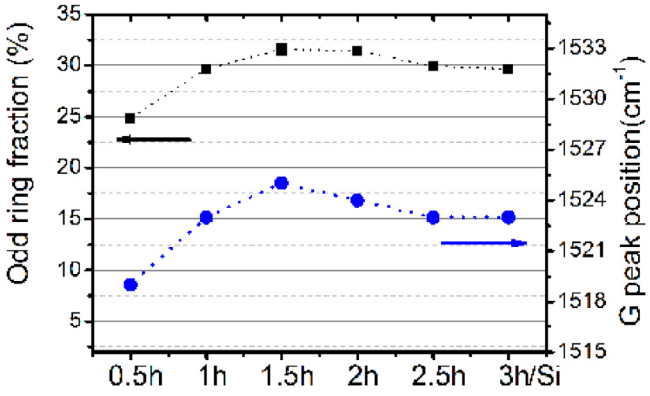

Fig. 6. odd ring fraction and G peak position of the samples on Si substrates with depositing time.

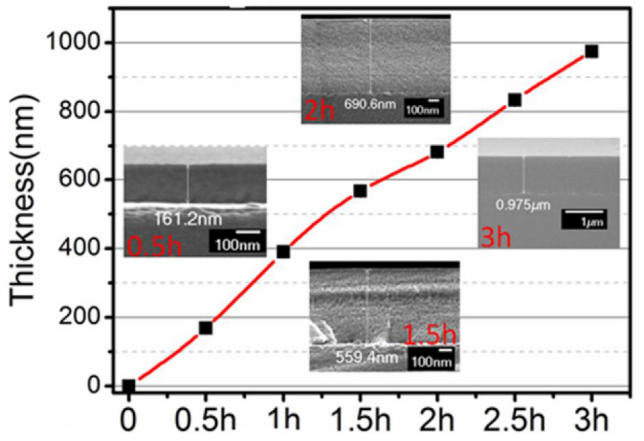

Fig. 7. Thickness of the samples on Si substrates with different deposition time.

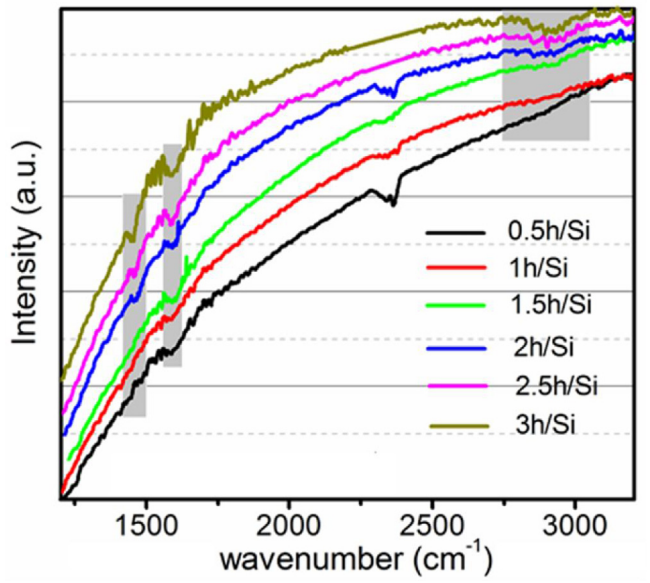

Fig. 8. FTIR results of the samples on Si substrates with different deposition time.

surface roughness (the steel ball roughness is about 0.025 μm, and the Si substrate roughness is <0.5 nm), in addition to their thickness effect. Thus, FTIR spectra can't reflects film bulk nature and recognize minor structural change when the Si substrate-samples can't have enough thickness. However, the peaks at 1600 cm^{-1} from sp^2 bond mixtures at 2 h, 2.5 and 3 h confirm the presence of FL clusters. The stronger C-H peaks partly mean higher hydrogen bonding in the films, coincide with the decrease of FL content at late deposition stage (Fig. 6). In a word, the Si substrate-film structure has to be revealed by a combination of Raman, FTIR, XPS and TEM etc. as shown in the Section 3.1.

3.4. The analysis for the structural evolution of the samples on steel balls and Si substrates

Based on the Characteristics in 3.2 and 3.3 section, the structural evolutions of the steel ball- and Si substrate- samples are shown as follows:

$$GL(0.5\,h/Fe, \downarrow) \rightarrow FL(\uparrow) \rightarrow FL(\rightarrow) \quad (1)$$

$$FL(0.5\,h/Si, \uparrow) \rightarrow FL(\rightarrow) \quad (2)$$

Here, ↓ is the content decrease, ↑ is the content increase, and → is the content relative stability. We suggest that the difference is probably correlated with material shape (sphere and flake) and deposition process. The diameter of steel ball is ~5 mm, and the Si substrate thickness is ~1 mm, which can cause the difference of energized ion deposition distances/direction from the two substrate surfaces (Fig. 9a and b). Fig. 9c shows the Raman spectra of the samples on steel balls and steel flakes with the same deposition condition. As the deposition time increases from 0.5 h to 1 h, the ball sample spectrum is almost the same with the flake one. This indicates that material shape is not a key factor.

Deposition process can play a key role, according to the comparation among the 0.5 h/Si flake sample' spectrum and the steel flake sample' one (Figs. 5a and 9c). For hydrogenated carbon films, the CHn^+ and H^+ enter easily into sublayer and cause higher compressive stress based on the subplantation model [2]. According to the studies about the growth of FL-C:H films on the Si substrates [21,22], the FL clusters with the incorpotation of such odd rings are not fully driven by thermodynamics, but is closely related to high compressive stress determined by ion bombardment in depositing process. The creation of such rings is a stress relaxation process, and easily bestows the film lower compressive stress [4,22,23]. It is worthy noted that at late deposition stage of 2 h, 2.5 h and 3 h, the steel ball- and Si substrate- samples have close FL content. This is a clue that they have similar FL formation mechanism at the late deposition process (Fig. 9d). Nevertheless, in this study, all the steel balls and Si substrates are not heated intendedly in the deposition process and their temperature increase due to the plasma heating effect. Noted that, in order to enhance the adhesion of carbon films on Fe substrates, the in-situ plasma nitriding (1200 V, 2 h) which is additionally used after Ar^+ etching (negative voltage of 1000 V, 20 min), can attribute to higher temperature of the steel substrate. After the nitriding and before the deposition of carbon films (1000 V, 2 h), the steel ball temperature is ~230 °C. As for the deposition process on Si substrate, the temperature is ~120 °C. The higher substrate temperature is benefit for the formation of GL clusters in the 0.5 h/Fe ball sample, since the higher substrate temperature without external heat treatment and catalysts is indispensable to form graphene sheets [24,25]. W.T. Zheng and coworkers [26] proposed by tight-binding molecular dynamics that the rapidly reduction in compressive stress may occur because GL carbon forms at 450 K (~177 °C). At the temperature, subplanted atoms migrate to the surface where they can form sp^2 layers via activated thermal diffusion, leading to the relaxation of stress (Fig. 9d). Namely, at the starting deposition (0.5 h), the GL layer formation can relieve high compressive stress. This is different from at the late deposition that odd rings need to be formed for the relief. The employed voltage decreases from 1200 V of the nitriding to 1000 V of the film deposition, thereby leading to the decline of

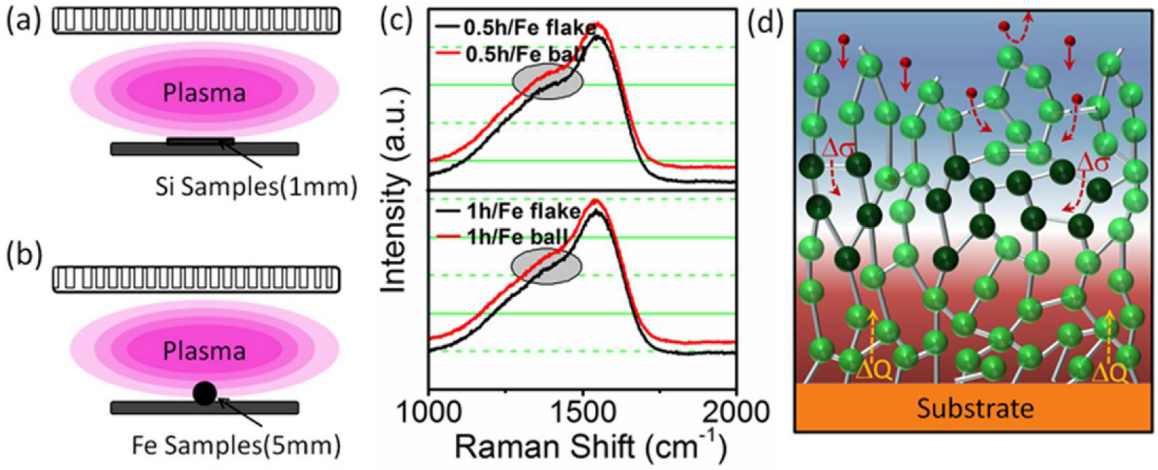

Fig. 9. Schematic of the film preparation process on a Si substrate (a) and steel ball (b); Raman spectra of the films on steel balls and flakes (c); Illustration of steel ball-film's structure evolution with depositing time.

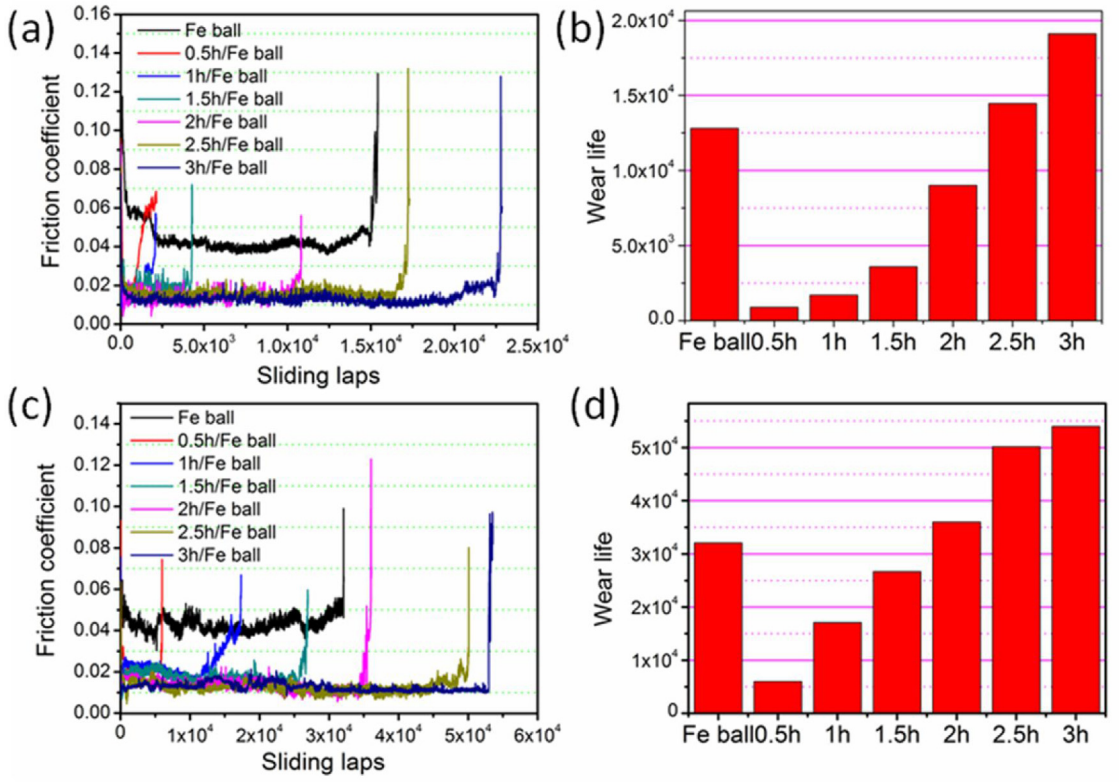

Fig. 10. Friction coefficients and wear lives of the 0.5 h/Si (a and b) and 1 h/Si (c and d) samples against steel ball and coated steel ball-ones.

Fe substrate temperature. This can explain that FL element is introduced into GL clusters with the increasing time from 0.5 h to 1.5. Overall, the (1) structural evolution on Fe balls may be result from the competition between high starting substrate temperature after the nitriding pre-process, and relaxation of high compressive stress from energized ion bombardment.

3.5. *The frictional behaviors of the samples on steel balls and Si substrates*

Because these films move toward tribological application, we investigate their frictional behaviors. Fig. 10a and c respectively show the friction coefficients (COFs) of the 0.5 h/Si and 1 h/Si films against all coated steel ball-samples as a function of sliding laps. All the film friction couples have lower COFs under ambient conditions with 25% relative humidity, as compared with the couples against uncoated Fe ball. Their wear lives has obvious differences. Based on the statistics about the wear life in Fig. 10b and d, the thickness can obviously affect these film wear lives. For example, for 0.5 h/Si film, only two friction couples have longer wear lives than the couple against Fe ball. As for 1 h/Si film, its increasing thickness can add a new friction couple. The wear life of 1 h/Si film against 3 h/Fe ball is prolonged from 3.2×10^4 cycles of 1 h/Si–Fe ball couple to 5.4×10^4 cycles. Meanwhile, a phenomenon is worthy noted that the friction couples containing high FL content have lower COFs. For example, the 0.5 h/Si film against coated 2 h/Fe, 2.5 h/Fe and

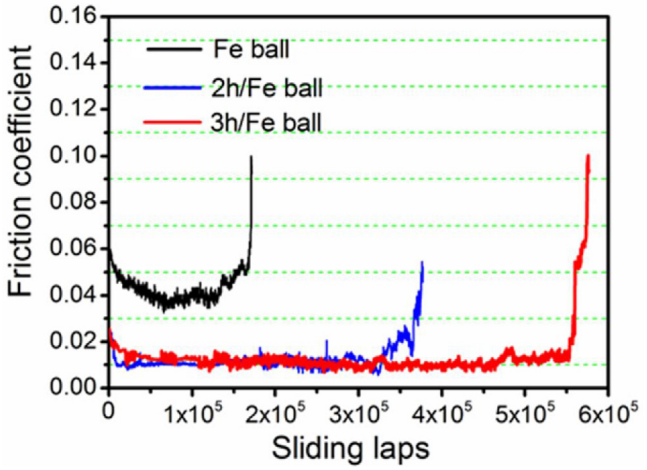

Fig. 11. Friction coefficients of the 3 h/Si sample against coated 2 h/Fe and 3 h/Fe ball samples.

3 h/Fe balls have steady COFs as low as 0.012. Moreover, with the increasing sliding laps, real-time super-low COFs ($\mu < 0.01$) can be achieved. As for 1 h/Si film, it against coated 2.5 h/Fe and 3 h/Fe balls exhibit super-low COFs. The results indicate that the FL structural film friction couples are an effective way to achieve ultra-low or super-low friction in open air.

We choose the couples, 3 h/Si film against coated 2 h/Fe and 3 h/Fe ball samples, as representatives to study the completely tribological behaviors of these films. The reason is that these films' thickness and FL content can affect their COFs and wear lives above. The 3 h/Si film is chosen due to its highest thickness. It also has a relative high FL content which is close to that of another Si substrate-sample apart from 0.5/Si film. The 2 h/Fe ball sample has a highest FL content and the 3 h/Fe ball one has a highest thickness. It can be seen that the couple of 3 h/Si against 2 h/Fe gets into a super-low COFs ($\mu = \sim 0.009$) state quickly compared to the couple of 3 h/Si against 3 h/Fe ($\mu = \sim 0.01$) (Fig. 11). Their wear lives are prolonged to 3.7×10^5 and 5.5×10^5 cycles (Fig. 11). The super-low friction mechanism is discussed in the following section 3.6. In addition, the film couples can attain super-low friction under lower load and velocity (5N and 0.05m/s) than those ($\geq$15 N and $\geq$0.12 m/s) for the FL structural films against Si_3N_4 or Al_2O_3 balls as reported in the studies [9,13]. Our result can widen the superlubricity scope for FL structural films in open air.

3.6. Raman analysis on the wear track and wear scar of the samples

According to the Characteristics in 3.2 and 3.3 section, Raman spectroscopy is an effective way to distinguish carbon structural change. As known, the initial friction materials are often quickly covered by carbon-rich layers. For the film friction couples, wear track and scars are two states of wear materials after friction. They experiences repeated strain and heat effects, and thus trigger structural transformation. Fig. 10 shows Raman fit results obtained at the wear track and wear scar of the couple of 3 h/Si against 3 h/Fe which has longest wear life and super-low COFs. The wear track of the 3 h/Si film has high odd ring fraction than its original film (Fig. 12a and c). The spectrum on wear scar of the 3 h/Fe film has two obvious shoulder peaks at 1200 and 1380 cm^{-1}. The 1200 cm^{-1} peak originates from heptagons in FL clusters. Corresponding four peaks' fit result of the wear scar shows an increase of odd ring fraction after friction. Herein, as discussed above, the higher odd ring fraction of the couple after friction indicates that FL structure is further formed at the frictional interface. This is consistent with our previous studies [13,14,27,28]. In addition, the film friction couples containing high FL content have lower COFs (Fig. 10). Thus, FL structure within the carbon film and the sliding induced at friction interface can be probably responsible for super-low friction in open air.

4. Conclusion

This study reports the nanostructure evolutions of a-C:H films on steel balls and Si substrates with depositing time. For the steel ball-films, their structures are GL structure at the starting deposition (0.5 h) and then transform into FL structure. As for the Si substrate-films, their structures are FL structure throughout the thickness. The evolution difference may be result from the competition between high substrate temperature from additional nitriding pre-process on the steel balls (is higher than that of the film deposition), and relaxation of compressive stress from energized ion bombardment in the film deposition. The FL structural film friction couples are more effective way to achieve ultra-low or super-low friction in open air, than the film against uncoated Fe ball. In particular, the Si substrate-film with 3 h, against the steel ball-film with 2 h and 3 h, exhibit super-low friction ($\sim$0.009) and superlong wear life ($\sim 5.5 \times 10^5$ cycles), showing promising potential as a prominent solid lubricating material in real applications. The excellent friction behaviors are closely linked with both FL structures within the carbon films and the sliding induced at friction interfaces. Our result can widen the superlubricity scope for FL structural films in

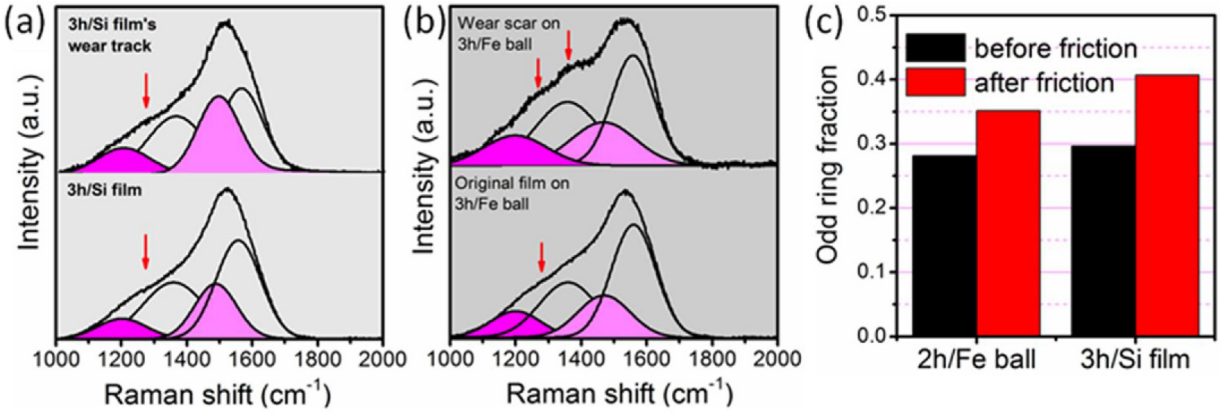

Fig. 12. Raman spectra (a and b) and odd ring fraction (c) of the 3 h/Si-3 h/Fe ball film friction couple before and after friction.

open air, namely, from previously high load and velocity (≥15 N and ≥0.12 m/s), to currently middle load and velocity (5N and 0.05m/s).

Acknowledgements

This work is supported by the Major State Basic Research Development Program of China (973 Program) (No 2013CB632304), and the National Natural Science Foundation of China (51475447, 51527901, 51611530704 and 51661135022) as well as CVS "Light of West China" Program.

References

[1] A.H. Lettington, Applications of diamond-like carbon thin films, Carbon 36 (1998) 555–560.
[2] J. Robertson, diamond-like amorphuos carbon, Mater. Sci. Eng. R 37 (2002) 129–281.
[3] A.C. Ferrari, J. Robertson, Resonant Raman spectroscopy of disordered, amorphous, and diamondlike carbon, Phys. Rev. B 64 (2001).
[4] M. Lejeune, M. Benlahsen, R. Bouzerar, Stress and structural relaxation in amorphous hydrogenated carbon films, Appl. Phys. Lett. 84 (2004) 344.
[5] Jin-Koog Shin, Churl Seung Lee, Kwang-Ryeol Lee, Kwang Yong Eun, Effect of residual stress on the Raman-spectrum analysis of tetrahedral amorphous carbon films, Appl. Phys. Lett. 78 (2001) 631–633.
[6] M.P. Siegal, D.R. Tallant, L.J. Martinez-Miranda, J.C. Barbour, R.L. Simpson, D.L. Overmyer, Nanostructural characterization of amorphous diamondlike carbon films, Phys. Rev. B 61 (2000) 10451–10462.
[7] Q. Wang, C. Wang, Z. Wang, J. Zhang, D. He, Fullerene nanostructure-induced excellent mechanical properties in hydrogenated amorphous carbon, Appl. Phys. Lett. 91 (2007) 141902.
[8] J.G. Buijnsters, M. Camero, R. Gago, A.R. Landa-Canovas, C. Gómez-Aleixandre, I. Jiménez, Direct spectroscopic evidence of self-formed C60 inclusions in fullerene-like hydrogenated carbon films, Appl. Phys. Lett. 92 (2008) 141920.
[9] C. Wang, S. Yang, Q. Wang, Z. Wang, J. Zhang, Super-low friction and super-elastic hydrogenated carbon films originated from a unique fullerene-like nanostructure, Nanotechnology 19 (2008) 225709.
[10] P. Wang, X. Wang, W. Liu, J. Zhang, Growth and structure of hydrogenated carbon films containing fullerene-like structure, J. Phys. D: Appl. Phys. 41 (2008) 085401.
[11] X. Wang, P. Wang, S. Yang, J. Zhang, Tribological behaviors of fullerene-like hydrogenated carbon (FL-C:H) film in different atmospheres sliding against Si3N4 ball, Wear 265 (2008) 1708–1713.
[12] L. Ji, H. Li, F. Zhao, W. Quan, J. Chen, H. Zhou, Effects of pulse bias duty cycle on fullerenelike nanostructure and mechanical properties of hydrogenated carbon films prepared by plasma enhanced chemical vapor deposition method, J. Appl. Phys. 105 (2009) 106113.
[13] Y. Wang, J. Guo, K. Gao, B. Zhang, A. Liang, J. Zhang, Understanding the ultra-low friction behavior of hydrogenated fullerene-like carbon films grown with different flow rates of hydrogen gas, Carbon 77 (2014) 518–524.
[14] Y. Wang, K. Gao, J. Zhang, Structure, mechanical, and frictional properties of hydrogenated fullerene-like amorphous carbon film prepared by direct current plasma enhanced chemical vapor deposition, J. Appl. Phys. 120 (2016) 045303.
[15] J. Wang, A. Liang, F. Wang, L. Xu, J. Zhang, Controllable preparation of fluorine-containing fullerene-like carbon film, Appl. Surf. Sci. 370 (2016) 291–296.
[16] J. Wang, Z. Cao, F. Pan, F. Wang, A. Liang, J. Zhang, Tuning of the microstructure, mechanical and tribological properties of a-C:H films by bias voltage of high frequency unipolar pulse, Appl. Surf. Sci. 356 (2015) 695–700.
[17] M. Chhowalla, Gehan A.J. Amaratunga, Thin films of fullerene-like MoS2 nanoparticles with ultra-low friction and wear, Nature 407 (2000) 164–167.
[18] J. Neidhardt, L. Hultman, Z. Czigány, Correlated high resolution transmission electron microscopy and X-ray photoelectron spectroscopy studies of structured CNx (0 < x < 0.25) thin solid films, Carbon 42 (2004) 2729–2734.
[19] R. Wächter, A. Cordery, Response surface methodology modelling of diamond-like carbon film deposition, Carbon 37 (1999) 1529–1537.
[20] Zs Czigaíny, I.F. Brunell, J. Neidhardt, L. Hultman, K. Suenaga, Growth of fullerene-like carbon nitride thin solid films consisting of cross-linked nano-onions, Appl. Phys. Lett. 79 (2001) 2639.
[21] Z. Wang, J. Zhang, Deposition of hard elastic hydrogenated fullerenelike carbon films, J. Appl. Phys. 109 (2011) 103303.
[22] Y. Wang, K. Gao, J. Shi, J. Zhang, Bond topography and nanostructure of hydrogenated fullerene-like carbon films: a comparative study, Chem. Phys. Lett. 660 (2016) 160–163.
[23] Q. Wang, C. Wang, Z. Wang, J. Zhang, D. He, The correlation between pentatomic and heptatomic carbon rings and stress of hydrogenated amorphous carbon films prepared by dc-pulse plasma chemical vapor deposition, Appl. Phys. Lett. 93 (2008) 131920.
[24] M. Chhowalla, A.C. Ferrari, J. Robertson, G.A.J. Amaratunga, Evolution of sp2 bonding with deposition temperature in tetrahedral amorphous carbon studied by Raman spectroscopy, Appl. Phys. Lett. 76 (2000) 1419–1421.
[25] C. Wang, D. Diao, X. Fan, C. Chen, Graphene sheets embedded carbon film prepared by electron irradiation in electron cyclotron resonance plasma, Appl. Phys. Lett. 100 (2012) 231909.
[26] B. Zheng, W.T. Zheng, S.S. Yu, H.W. Tian, F.L. Meng, Y.M. Wang, J.Q. Zhu, S.H. Meng, X.D. He, J.C. Han, Growth of tetrahedral amorphous carbon film: tight-binding molecular dynamics study, Carbon 43 (2005) 1976–1983.
[27] Y. Wang, J. Guo, J. Zhang, Y. Qin, Ultralow friction regime from the in-situ production of a richer fullerene-like nanostructured carbon in sliding contact, RSC Adv. 5 (2015) 106476.
[28] J. Guo, Y. Wang, H. Liang, A. Liang, J. Zhang, Mechanical properties and tribological behavior of fullerene-like hydrogenated carbon films prepared by changing the flow rates of argon gas, Appl. Surf. Sci. 364 (2016) 288–293.